Cation-Dependent Fluorescent Properties of Naphthalimide Derivatives with *N*-Benzocrown Ether Fragment

Pavel A. Panchenko,[†] Yuri V. Fedorov,[†] Valeri P. Perevalov,[‡] Gediminas Jonusauskas,[§] and Olga A. Fedorova*[,†,‡]

A. N. Nesmeyanov Institute of Organoelement Compounds, Russian Academy of Sciences, Vavilova Street 28, Moscow, 119991, Russia, Mendeleev University of Chemical Technology of Russia, Miusskaya Square 9, Moscow, 125047, Russia, and, Centre de Physique Moléculaire Optique et Hertzienne (CPMOH), UMR CNRS 5798, Université Bordeaux 1, 351, Cours de la Libération, 33405 Talence, France

Received: October 30, 2009; Revised Manuscript Received: December 27, 2009

The investigation of *N*-phenyl-4-amino- and *N*-phenyl-4-acetamido-1,8-naphthalimides containing *N*-benzo-15-crown-5 ether substituent showed that the presence of ionophoric fragment as *N*-substituent in naphthalimide molecule provides the design of compound possessing the properties of fluorescent receptor. The addition of metal cations does not change the position of absorption and emission bands but substantial increases the fluorescence intensity. The study of molecules included the theoretical and experimental (optical, NMR) methods, analysis of intramolecular charge (electron) transfer and fluorescence properties in the presence and absence of metal ions.

Introduction

Derivatives of 1,8-naphthalimides have been widely used as the photoinduced electron transfer (PET) or photoinduced charge transfer (ICT) type fluoroionophores.[1,2] These compounds have found application in the construction of fluorosensors. It is understood from the abundance of literature on this topic that intramolecular PET and ICT are the most commonly exploited mechanisms to elucidate observed physical−chemical phenomena. In the presence of guest species, the guest-induced modulations in the extent of PET or ICT govern the nature of the output signal of the molecular system; it may lead to fluorescence enhancement or quenching, depending on the sensor design.

Chemosensors can and do find employment in many disciplines such as biochemistry, clinical and medical sciences, analytical chemistry, and environmental science. In lines of development of chemosensors, the search for selective and sensitive fluorescent probes for metal ions has tremendously gained importance.[3−6]

The examples of chemosensors based on naphthlimide derivatives are presented in the literature. pH-dependent fluorescence was found for amino-substituted naphthalimides, which emulates the unidirectional, path-selective PET of the bacterial photosynthetic reaction center (PRC).[7] Piperazine-substituted naphthalimide compounds also demonstrated characteristic pH fluorescent probe properties, whereas the piperidine and polyamine derivatives possess selectivity toward Ag^+ and Cu^{2+} ions.[8−10] Novel yellow-green emitting 1,8-naphthalimides, containing a 4-amino-2,2,6,6-tetramethylpiperidinyl moiety, were configured as "fluorophore−spacer−receptor" systems.[11,12] The presence of metal ions (Cu^{2+}, Zn^{2+}, Pb^{2+}, Ni^{2+}) and protons was found to make impossible PET resulting in enhanced fluorescence intensity. The monomeric *N*,*N*-dimethylaminoethylene-*N*-allyl-1,8-naphthalimide and methylmethacrylate-based copolymer including *N*,*N*-dimethylaminoethylene-*N*-allyl-1,8-naphthalimide were found to be the fluorophores that can be used as homogeneous PET fluorescent sensors exhibiting fluorescence enhancement induced by metal ions (Fe^{2+}, Zn^{2+}, Pb^{2+}, Ni^{2+}).[13−15] The design, synthesis, and photophysical evaluation of *N*-butyl-4-[di-(2-picolyl)amino]-5-(2-picolyl)amino-1,8-naphthalimide showed that this compound was suitable for the detection of Zn^{2+} in aqueous acetonitrile solution at pH 7.0.[16]

Some examples of crown-ether-containing naphthalimides designed as fluorescent chemosensors for heavy and transition metal cations are also known.[17−22]

The main design particularity of all of the naphthalimide derivatives described above is that the receptor unit is located as the substituent in the 4-position. Only recently have naphthalimide derivatives containing an ionophoric fragment as the substituent at the *N*-atom of the imide fragment been studied by Michael D. Heagy and coauthors.[23] Also, in our previous work[24] we described the synthesis of the naphthalimide derivatives **1a,b** (see Scheme 1). The change of the position of the crown ether fragment from the naphthalene part to the composition of *N*-aryl substituent leads to substantial structural features. Thus, compound **1a** combines donor amino group−acceptor naphthalimide residue−donor benzocrown ether fragment (D_1-A-D_2). As a result of the presence of two donor sites, the molecule can serve as a model for a two-direction photoinduced charge transfer process. Naphthalimide has a unique

SCHEME 1: Chemical Structure of Naphthalimides 1a,b

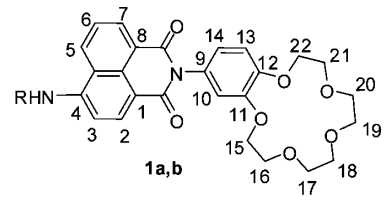

1a: R = H, **1b**: R = COMe

* To whom correspondence should be addressed. E-mail: fedorova@ineos.ac.ru. Tel.: +7 (499) 135 8098. Fax: +7 (499) 135 5085.
[†] Russian Academy of Sciences.
[‡] Mendeleev University of Chemical Technology of Russia.
[§] Université Bordeaux 1.

10.1021/jp9103728
Published on Web 02/25/2010

characteristic in its frontier molecular orbitals (MOs): a vertical nodal plane passes through the two central carbon atoms in the naphthalene ring and the nitrogen atom.[25] Because of this symmetry, the electronic interaction between naphthalimide and the donor attached to the nitrogen atom through the spacers is minimized. Complex formation through the crown ether does not exhibit a remarkable effect on optical characteristics.

In the compound **1b**, the amino group is replaced by a weaker donor amido substituent. Thus, if two benzocrown ethers (D_2) and naphthalimide residue (A) are deconjugated, PET between D_2 and A fragments becomes the main photoinduced process. In this case, the substantial optical changes upon complex formation can be suggested. In this paper, we present a detailed theoretical and experimental study of the electronic properties of the naphthalimide derivatives shown in Scheme 1.

The observation of molecules **1a,b** includes the analysis of the electron transfer process in the presence and absence of metal ions aimed to determine the ability of molecules to be fluorescent sensors. Complexation studies were performed using magnesium and barium divalent cations as their perchlorate salts. These two alkaline earth metal ions were chosen because they have a high affinity for crown ether moiety in solution and they display very different ionic radii (Mg^{2+} − 0.78 Å; Ba^{2+} − 1.43 Å), which should induce the formation of distinct complex structures.

Experimental Methods

Materials. The detailed synthesis of crown ether-containing naphthalimides **1a** and **1b** has been described elsewhere.[24] Anhydrous $Mg(ClO_4)_2$, $Ba(ClO_4)_2$, and spectrophotometric-grade acetonitrile (Aldrich) were used as received.

Optical Measurements. The absorption spectra were taken on a Varian-Cary 5G spectrophotometer. The fluorescence quantum yield measurements were performed using a Varian-Cary 5G spectrophotometer and a FluoroMax-3 spectrofluorimeter. Concentrations of solutions of about $0.5-2.0 \times 10^{-6}$ mol/L were used for the spectral measurements. All measured fluorescence spectra were corrected for the nonuniformity of detector spectral sensitivity. Quinine sulfate in 1*N* H_2SO_4 ($\varphi^{fl} = 0.55$)[26] and rhodamine 6G in ethanol ($\varphi^{fl} = 0.95$)[27] were used as references for the fluorescence quantum yield measurements.

Equilibrium Constant Determination. Complex formation of dye **1a,b** with Mg^{2+} and Ba^{2+} cations in acetonitrile at 20 ± 1 °C was studied by spectrofluorometric titration. The ratio of dye **1a** or **1b** to Mg^{2+}, Ba^{2+} was varied by adding aliquots of a solution of corresponding salt of known concentration to a solution of ligands **1a,b** of known concentration. The fluorescence spectrum of each solution was recorded, and the stability constants of the complexes were determined using the SPECFIT/32 program (Spectrum Software Associates, West Marlborough, MA). The following equilibria were considered in the fitting (L = **1a,b**; M = Mg^{2+}, Ba^{2+}):

• for complex formation with Mg^{2+} cations:

$$L + M \overset{K_{11}}{\rightleftharpoons} LM \qquad K_{11} = \frac{[LM]}{[L]\cdot[M]}$$

• for complex formation with Ba^{2+} cations:

$$L + M \overset{K_{11}}{\rightleftharpoons} LM \qquad K_{11} = \frac{[LM]}{[L]\cdot[M]}$$

$$2L + M \overset{K_{21}}{\rightleftharpoons} L_2M \qquad K_{21} = \frac{[L_2M]}{[L]^2\cdot[M]}$$

The stability constant for (**1a**)·Mg^{2+} was not determined because of the negligible changes in its fluorescence spectra upon complex formation. The fluorescence spectral shapes of the free ligands **1a,b** and their complexes LM and L_2M with Ba^{2+} cations were also calculated using the SPECFIT/32 program.

Determination of Fluorescence Quantum Yields of Complexes. The fluorescence quantum yields of complexes LM (*L* = **1a,b**; *M* = Mg^{2+}, Ba^{2+}) were determined using solutions of ligands **1a,b** in CH_3CN containing an excess of metal perchlorates in order to obtain 90−95% of ligand bound with the cation. The required metal excess was calculated from the known stability constants using the SPECFIT/32 program. In the case of L_2M complexes, the direct quantum yield determination was impossible because the presence of considerable amounts of other fluorescent species (L and LM) might not be avoided at any metal to ligand ratio. The quantum yields of L_2M complexes were estimated using the known quantum yields of L or LM and the ratio of areas underneath the calculated fluorescence spectra of the individual components L, LM, and L_2M.

Computational Details. Quantum chemical calculations were carried out by the MOPAC 2007 program package using the PM6 semiempirical method.[28] CI calculations were performed at optimized geometries, which reached gradient variations less than 0.01 kcal/mol. The solvent effect was included in geometry optimizations following the "COnductorlike Screening MOdel" (COSMO) implemented in MOPAC 2007. A dielectric constant of $\varepsilon = 40$ and a refraction index of solvent such that $n^2 = 2$ were used. The CI included eight occupied and eight unoccupied MOs.

NMR Experiments. The ^1H NMR spectra were recorded on a Varian-XR-400 spectrometer, operating at 400.13 MHz. The measurements were carried out in CD_3CN solution. The chemical shifts (given as δ in ppm) were referenced to hexamethyldisiloxane (HMDSO). The assignment of proton signals H(5) and H(7) is based on theoretical calculations, which were made using the ACD/Laboratories 6.0 program package.

***Compound* 1a.** $C_L = 1.6 \times 10^{-3}$ mol·L^{-1}. ^1H NMR (CD_3CN, 45 °C, δ, ppm, *J*/Hz): 3.62−3.71 (m, 8H, CH_2(17), CH_2(18), CH_2(19), CH_2(20)), 3.75−3.80 (m, 2H, CH_2(16)), 3.81−3.86 (m, 2H, CH_2(21)), 4.01−4.06 (m, 2H, CH_2(15)), 4.14−4.18 (m, 2H, CH_2(22)), 5.82 (brs, 2H, NH_2), 6.82 (dd, 1H, H(14), J = 2.3, J = 8.3), 6.88 (d, 1H, H(10), J = 2.3), 6.92 (d, 1H, H(3), J = 8.3), 7.02 (d, 1H, H(13), J = 8.3), 7.64 − 7.70 (m, 1H, H(6)), 8.27 (d, 1H, H(2), J = 8.3), 8.34 (d, 1H, H(7), J = 7.3), 8.49 (d, 1H, H(5), J = 8.6).

***Compound* 1b.** $C_L = 1.2 \times 10^{-3}$ mol·L^{-1}. ^1H NMR (CD_3CN, 30 °C, δ, ppm, *J*/Hz): 2.29 (s, 1H, CH_3CO), 3.62−3.71 (m, 8H, CH_2(17), CH_2(18), CH_2(19), CH_2(20)), 3.74−3.79 (m, 2H, CH_2(16)), 3.81−3.85 (m, 2H, CH_2(21)), 3.97−4.05 (m, 2H, CH_2(15)), 4.14−4.18 (m, 2H, CH_2(22)), 6.85 (dd, 1H, H(14), J = 2.3, J = 8.3), 6.91 (d, 1H, H(10), J = 2.3), 7.03 (d, 1H, H(13), J = 8.3), 7.79−7.87 (m, 1H, H(6)), 8.27−8.35 (m, 1H, H(3)), 8.46−8.58 (m, 3H, H(2), H(5), H(7)), 8.82 (brs, 1H, NHCO).

***Complex* (1a)·Mg^{2+}.** $C_L = 1.6 \times 10^{-3}$ mol·L^{-1}. Metal to ligand ratio M:L = 2:1. ^1H NMR (CD_3CN, 22 °C, δ, ppm, *J*/Hz): 3.89−4.01 (m, 8H, CH_2(17), CH_2(18), CH_2(19), CH_2(20)), 4.03−4.09 (m, 2H, CH_2(16)), 4.09−4.17 (m, 2H, CH_2(21)), 4.35−4.44 (m, 2H, CH_2(15)), 4.49−4.56 (m, 2H, CH_2(22)), 6.01 (brs, 2H, NH_2), 6.93 (d, 1H, H(3), J = 8.3), 7.13 (dd, 1H, H(14), J = 2.2, J = 8.3), 7.21 (d, 1H, H(10), J = 2.2), 7.30 (d, 1H, H(13), J = 8.3), 7.67−7.73 (m, 1H, H(6)), 8.27 (d, 1H, H(2), J = 8.3), 8.39 (d, 1H, H(7), J = 7.3), 8.50 (d, 1H, H(5), J = 8.6).

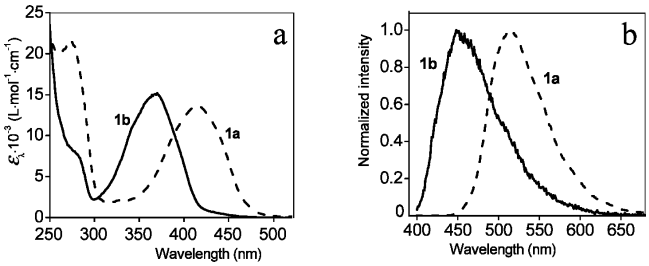

Figure 1. Absorption (a) and normalized emission (b) spectra of compounds **1a,b** in CH_3CN.

TABLE 1: Steady-State Absorption and Fluorescence Data and Stability Constants for Dyes 1a,b and Their Complexes with Mg^{2+} and Ba^{2+} Cations

	λ^{abs}_{max} (nm)	$\epsilon_\lambda \times 10^{-3}$ (L·mol^{-1}·cm^{-1})	λ^{fl}_{max} (nm)	φ^{fl}	lg K (M^{-1} or M^{-2})
1a	414	13.7	519	0.43	
(**1a**)·Mg^{2+}	417	14.0	521	0.49	not determined
(**1a**)$_2$·Ba^{2+}	415[a]	24.0[a]	539[b]	0.092	11.5 ± 0.2
(**1a**)·Ba^{2+}	417[a]	14.2[a]	522[b]	0.45	5.46 ± 0.09
1b	366	15.1	456	0.003	
(**1b**)·Mg^{2+}	368	15.1	454	0.61	5.33 ± 0.02
(**1b**)$_2$·Ba^{2+}	366[a]	24.0[a]	473[b]	0.051	10.28 ± 0.05
(**1b**)·Ba^{2+}	368[a]	14.7[a]	454[b]	0.071	4.58 ± 0.05

[a] Calculated from the spectrophotometric titration data and corresponding stability constants using the SPECFIT/32 program. [b] Calculated from the spectrofluorometric titration data using the SPECFIT/32 program.

***Complex* (1b)·Mg^{2+}.** $C_L = 1.2 \times 10^{-3}$ mol·L^{-1}. Metal to ligand ratio M:L = 2:1. ^{1}H NMR (CD_3CN, 45 °C, δ, ppm, *J*/Hz): 2.30 (s, 1H, CH_3CO), 3.93−4.03 (m, 8H, CH_2(17), CH_2(18), CH_2(19), CH_2(20)), 4.09 − 4.13 (m, 2H, CH_2(16)), 4.13−4.19 (m, 2H, CH_2(21)), 4.41−4.45 (m, 2H, CH_2(15)), 4.53−4.58 (m, 2H, CH_2(22)), 7.17 (dd, 1H, H(14), $J = 2.3$, $J = 8,6$), 7.24 (d, 1H, H(10), $J = 2.3$), 7.33 (d, 1H, H(13), $J = 8.6$), 7.86 (dd, 1H, H(6), $J = 7.3$, $J = 8.6$), 8.35 (d, 1H, H(3), $J = 8.1$), 8.52 (d, 1H, H(2), $J = 8.1$), 8.56 (d, 1H, H(7), $J = 7.3$), 8.57 (d, 1H, H(5), $J = 8.6$), 8.79 (brs, 1H, NHCO).

Results and Discussion

Steady-state absorption and fluorescence characteristics of **1a,b** measured in acetonitrile solution are presented in Figure 1a,b and Table 1. Compounds **1a,b** display absorption corresponding to the charge transfer transition in the 1,8-naphthalimide moieties from the electron-donating amino or amido substituent at the C-4 position to the carbonyl groups. The decrease of electron-donating property of the substituent at C-4 going from amino to amido group results in a 50 nm hypsochromic shift of the lowest energy absorption band of **1b** relative to **1a** (Figure 1).

The emission of **1a,b** in the visible region with well-pronounced maxima at 519 and 456 nm correspondingly was observed in acetonitrile solutions. The fluorescence quantum yields were calculated relative to quinine sulfate in 1*N* H_2SO_4 ($\varphi^{fl} = 0.55$)[26] and rhodamine 6G in ethanol ($\varphi^{fl} = 0.95$)[27] as reference compounds. As it is seen (Table 1), the fluorescence quantum yield of **1a** is high, whereas **1b** shows considerably lower fluorescence quantum yield.

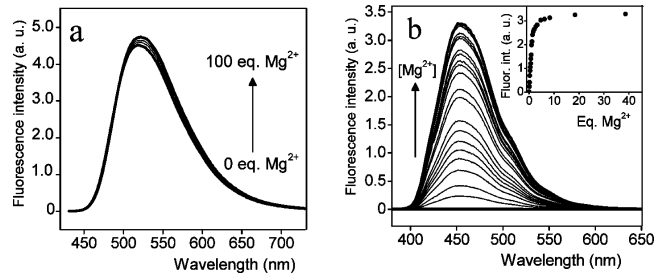

Figure 2. The changes in fluorescence of **1a** (a) and **1b** (b) in the presence of a graduated amount of $Mg(ClO_4)_2$ in CH_3CN solution. (a) $C_L = 1.3 \times 10^{-5}$ mol·L^{-1}, $\lambda_{ex} = 365$ nm; (b) $C_L = 8.2 \times 10^{-6}$ mol·L^{-1}, $\lambda_{ex} = 415$ nm. The inset shows fluorescence intensity at 454 nm versus equivalents of Mg^{2+}.

The addition of magnesium or barium perchlorates to the acetonitrile solutions of ligands **1a,b** does not lead to significant changes in positions of absorption and fluorescence bands but results in pronounced increasing of fluorescence intensity (Figure 2). The fluorescence enhancement was assigned to coordination of a cation with crown ether moiety, and was applied for calculation of stability constants (Experimental Methods).

The NMR analysis clearly confirmed the formation of complexes (Table 2). The addition of Mg^{2+} cations causes the downfield shift of the resonance proton signals of *N*-benzocrown ether part. The positions of the other proton signals stay unchanged. These results are in good agreement with the optical data demonstrating only small changes in optical characteristics of the chromophoric part of ligands **1a,b**.

To elucidate the mechanism of the charge transfer process, the quantum chemical calculations of highest occupied MO to lowest unoccupied MO (HOMO−LUMO) orbitals were carried out using MOPAC 2007, method PM6. The frontier orbital pictures for compounds **1a** and **1b** are shown in Figure 3. In the ground state (HOMO) of **1a**, the lone pair on the nitrogen atom is localized over the amino group. In the excited state (LUMO), the electron density is found to be shifted away from the nitrogen atom toward the acceptor naphthalimide moiety, which is expected for the charge transfer phenomenon. In the complex (**1a**)·Mg^{2+}, the HOMO and LUMO orbitals are very similar to **1a**, confirming the same charge transfer transition from amino group to carbonyl groups of naphthalimide fragment. Thus, the formation of a complex of Mg^{2+} with the ligand **1a** does not substantially affect the optical characteristics, a feature we have observed experimentally.

The electron density distribution in the frontier orbitals of **1b** is different. The decrease of the electron-donating character of the C-4 substituent in **1b** arising from the acylation of amino group shifts down the naphthalimide local MO energy levels of **1b** with respect to those in **1a**. As a result, the HOMO in **1b** appears to be located on the *N*-aryl fragment, which is not affected by structural and electronic changes in naphthalimide moiety (Figure 4). Yet it is obvious that optical transition

TABLE 2: Changes in the ^{1}H NMR Spectra of 1a,b Induced by the Presence of $Mg(ClO_4)_2$ in CD_3CN Solution[a]

hydrogen position		H(17,18,19,20)	H(16)	H(21)	H(15)	H(22)	H(14)	H(10)	H(13)
$\Delta\delta$ (ppm)[a]	compound **1a**	0.28	0.28	0.29	0.36	0.37	0.31	0.33	0.28
	compound **1b**	0.31	0.34	0.33	0.42	0.40	0.32	0.33	0.30

[a] $\Delta\delta = \delta_{complex} - \delta_{ligand}$.

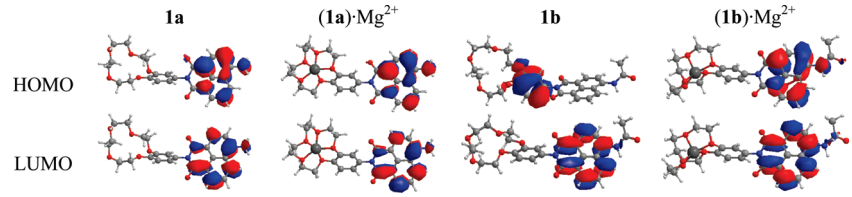

Figure 3. MOs of **1a**, (**1a**)·Mg^{2+}, **1b**, and (**1b**)·Mg^{2+} (HOMO and LUMO).

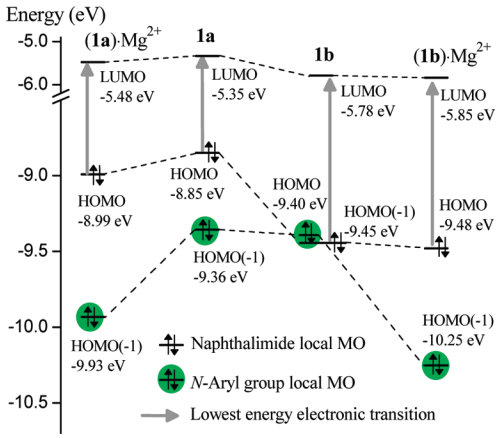

Figure 4. Energy levels of MOs of **1a**, (**1a**)·Mg^{2+}, **1b**, and (**1b**)·Mg^{2+}.

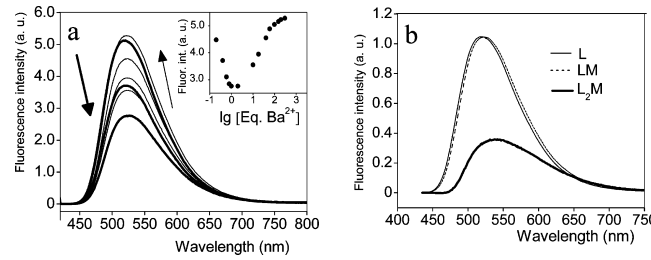

Figure 5. (a) The changes in fluorescence of **1a** in the presence of a graduated amount of $Ba(ClO_4)_2$ in CH_3CN solution. $C_L = 5.2 \times 10^{-6}$ mol·L^{-1}, $\lambda_{ex} = 415$ nm. The inset shows fluorescence intensity at λ^{fl}_{max} versus lg [Eq. Ba^{2+}]. (b) The calculated emission spectra of the free ligand **1a** and its 1:1 and 2:1 complexes with Ba^{2+} cations.

TABLE 3: The Dihedral Angle between the Naphthalimide Moiety and the *N*-Aryl Group in Compounds 1a,b and Their Complexes with Mg^{2+} Cations

	1a	(**1a**)·Mg^{2+}	**1b**	(**1b**)·Mg^{2+}
angle, °	89	41	89	89

responsible for the absorption band at 366 nm is not related to the HOMO located on the *N*-aryl group. The optical transition appears between HOMO(−1) and the LUMO in this case. The situation is reversed for (**1b**)·Mg^{2+}, where the HOMO is localized over the naphthalimide ring. This could be easily understood from the fact that the binding of cations with the crown ether receptor results in lowering the energy levels of *N*-aryl MOs, while the orbitals of the naphthalimide fragment remain unchanged.

The observed changes in the frontier orbital disposition are in conformity with the absence of π-electronic interaction between the naphthalimide moiety and the *N*-aryl fragment in the ground state of the compounds under study, which is in accordance with the negligible changes in the position of absorption and fluorescence maxima upon complex formation. The optimized ground-state geometries showing a high dihedral angle value between the naphthalimide moiety and benzene ring give evidence of this fact (see Table 3).

One can also conclude that the quenching of the fluorescent excited state of naphthalimide could be achieved by both increasing the energy of *N*-aryl orbitals (i.e., the introduction of electron-donating groups in the *N*-phenyl substituent) and lowering the energy levels of orbitals localized over the naphthalimide ring. Thus, the complex formation of **1b** with Mg^{2+} cations results in fluorescence enhancement, whereas the acylation of the amino group in **1a** to produce **1b** gives rise to a reduction of emission intensity.

The reason for the fluorescence quenching becomes clear after the analysis of Figure 4 we provided above. In the case of compound **1b**, the only compound exhibiting quenched fluorescence, the lowest energy absorptive electronic transition still remains (as for three other cases) located on naphthalimide and corresponds to a HOMO(−1) → LUMO transition. Once one electron is displaced to a higher laying orbital of naphthalimide, a fast electron transfer from the HOMO (located on *N*-aryl group) to the singly occupied HOMO(−1) (located on naphthalimide) takes place. The vertical emissive electronic transition located on naphthalimide becomes forbidden, and the system must relax in a nonradiative way: most probably this relaxation is associated with the electron transfer from the LUMO (located on naphthalimide) to the singly occupied HOMO (located on the *N*-aryl group).

The fluorescence effects induced by the presence of Ba^{2+} cations are different for compounds **1a** and **1b**. In the case of compound **1a**, the addition of a small amount of Ba^{2+} cations causes a shift of emission maximum to a longer wavelength region and a decrease of fluorescence intensity (see Figure 5a). Further increasing of the amount of Ba^{2+} leads to the return of the fluorescence band position as well as the recovery of fluorescence intensity. The observed optical effects are related to the formation of different types of complexes. Thus, first at low Ba^{2+} concentration, the formation of a sandwich complex

SCHEME 2: The Structure of Complexes of 1a,b with Ba^{2+} Cations

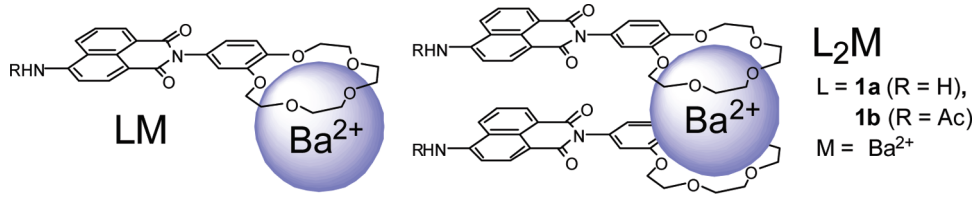

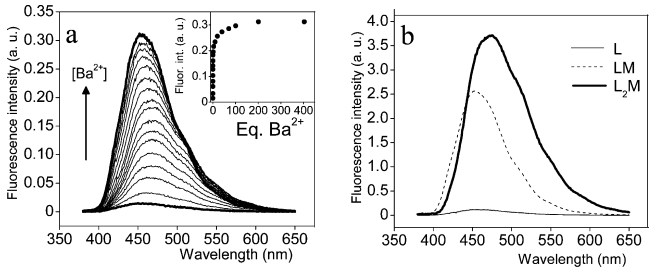

Figure 6. (a) The changes in fluorescence of **1b** in the presence of a graduated amount of $Ba(ClO_4)_2$ in CH_3CN solution. $C_L = 1.3 \times 10^{-5}$ mol·L^{-1}, $\lambda_{ex} = 365$ nm. The insert shows fluorescence intensity at λ^{fl}_{max} versus equivalents of Ba^{2+}; (b) The calculated emission spectra of the free ligand **1b** and its 1:1 and 2:1 complexes with Ba^{2+} cations.

is observed. If the **1a** molecules in this complex are arranged as a small H-aggregate with mutual disposition of molecules, intermolecular excimer formation could be suggested. An intramolecular excimer formed from two naphthalimides linked together by a polymethylene chain was reported previously.[29,30] In our case, two types of noncovalent interactions participate in the formation of a stacking dimeric complex, namely, sandwich complexing through the interaction of cations of large size with crown ether moiety and stacking interaction occurring between two large conjugated systems upon their close disposition (Scheme 2). This explains the bathochromic shift and the decrease of fluorescence intensity. The excess of Ba^{2+} cations causes the formation of complex composition (**1a**)·Ba^{2+}, which possesses the fluorescence characteristics closed to those for initial **1a** (see Figure 5a,b).

The addition of a graduated amount of Ba^{2+} to the acetonitrile solution of **1b** leads to the increase of fluorescence intensity with a concomitant change of fluorescence band position (see Figure 6a). The initial fluorescence quenching like in the case of **1a** is not observed as the emission intensity of complex (**1b**)$_2$·Ba^{2+} is higher than that for the free ligand (see Figure 1b). The former circumstance is evident if we take into consideration the spectacular changes of emission intensity of **1b** caused by the complexation when compared with those for compound **1a** (see the quantum yields of **1a,b** and their complexes in Table 1). Thus, the excimer formation, which is in response to the fluorescence quenching in the sandwich complex (**1b**)$_2$·Ba^{2+}, is not capable of overcoming the pronounced effect of enhancement of emission intensity. The increase of fluorescence for complex (**1b**)·Ba^{2+} is similar to the one observed for the Mg^{2+} complex of **1b**, whereas the magnitude of effect is substantially lower. This could be due to the low charge density on Ba^{2+} cation, leading to less significant HOMO energy lowering of the complexed *N*-aryl molecular fragment as compared with the Mg^{2+} complex and consequently reducing (but not completely forbidding) electron transfer as a result.

Conclusions

An efficient electron transfer between naphthalimide and benzocrown ether fragments of compounds **1a,b** takes place in the absence of metal ions, leading to fluorescence quenching. In the presence of metal ions, the lone pair of electrons originally involved in the electron transfer process is engaged in metal ion binding suppressing electron transfer process. As a result the fluorescence enhancement is observed upon complexation with metal ions.

The investigation of *N*-phenyl-4-amino- (**1a**) and *N*-phenyl-4-acethylamino- (**1b**) 1,8-naphthalimides containing *N*-benzo-15-crown-5 ether substituent showed that the presence of an ionophoric fragment as the *N*-substituent in the naphthalimide molecule provides the design of a compound possessing the properties of a fluorescent receptor. The addition of metal cations does not change the position of absorption and emission bands but substantially changes the fluorescence intensity. Through the studied molecules, the *N*-acethylamino derivative **1b** looks more promising because the low fluorescent initial ligand becomes highly fluorescent in the presence of metal ions.

Acknowledgment. This work was supported by the Russian Foundation for Basic Research (Project 09-03-0047, 09-03-93116), PICS 3904, and program of the Russian Academy of Sciences.

References and Notes

(1) Burdette, S. C.; Walkup, G. K.; Spingler, B.; Tsien, R. Y.; Lippard, S. J. *J. Am. Chem. Soc.* **2001**, *123*, 783–17841.
(2) Fan, J.; Peng, X.; Wu, Y.; Lu, E.; Hou, J.; Zhang, H.; Zhang, R.; Fu, X. *J. Luminesc.* **2005**, *114*, 125–130.
(3) de Silva, A. P.; Gunaratne, H. Q. N.; Gunnlaugsson, T.; Huxley, A. J. M.; McCoy, C. P.; Rademacher, J. T.; Rice, T. E. *Chem. Rev.* **1997**, *97*, 1515–1566.
(4) *Fluorescent Chemosensors for Ion and Molecular Recognition*; Czarnik, A. W., Ed.; American Chemical Society: Washington, DC, 1993.
(5) Gründler, P. *Chemical Sensors: An Introduction for Scientists and Engineers*; Springer-Verlag: Berlin/Heidelberg/New York, 2007; pp 199−225.
(6) Valeur, B.; Leray, I. *Coord. Chem. Rev.* **2000**, *205*, 3–40.
(7) de Silva, A. P.; Rice, T. E. *Chem. Commun.* **1999**, 163–164.
(8) Gan, J.; Chen, K.; Chang, C.-P.; Tian, H. *Dyes Pigm.* **2003**, *57*, 21–28.
(9) Li, Z.-Z.; Niu, C.-G.; Zeng, G.-M.; Liu, Y.-G.; Gao, P.-F.; Huang, G.-H.; Mao, Y.-A. *Sens. Actuators, B* **2006**, *114*, 308–315.
(10) Jia, L.; Zhang, Y.; Guo, X.; Qia, X. *Tetrahedron Lett.* **2004**, *45*, 3969–3973.
(11) Bojinov, V. B.; Panova, I. P. *Dyes Pigm.* **2009**, *80*, 61–66.
(12) Bojinov, V. B.; Panova, I. P.; Chovelon, J.-M. *Sens. Actuators, B* **2008**, *135*, 172–180.
(13) Grabchev, I.; Chovelon, J.-M.; Qian, X. *J. Photochem. Photobiol., A* **2003**, *158*, 37–43.
(14) Grabchev, I.; Chovelon, J.-M. *Dyes Pigm.* **2008**, *77*, 1–6.
(15) Staneva, D.; Grabchev, I.; Soumillion, J.-P.; Bojinov, V. *J. Photochem. Photobiol., A* **2007**, *189*, 192–197.
(16) Cui, J.; Zhang, R.; Xu, Z.; Qian, X. *Tetrahedron* **2006**, *62*, 10117–10122.
(17) Mu, H.; Gong, R.; Ma, Q.; Sun, Y.; Fu, E. *Tetrahedron Lett.* **2007**, *48*, 5525–5529.
(18) Rurack, K.; Resch-Genger, U.; Bricks, J. L.; Spieles, M. *Chem. Commun.* **2000**, 2103–2104.
(19) Bricks, J. L.; Kovalchuk, A.; Trieflinger, C.; Nofz, M.; Bufschel, M.; Tolmachev, A. I.; Daub, J.; Rurack, K. *J. Am. Chem. Soc.* **2005**, *127*, 13522–13529.
(20) He, H.; Mortellaro, M. A.; Leiner, M. J. P.; Fraatz, R. J.; Tusa, J. K. *J. Am. Chem. Soc.* **2003**, *125*, 1468–1469.
(21) Anikin, V. F.; Fedko, N. F. *Russ. J. Org. Chem.* **2006**, *42*, 73–76.
(22) Cosnard, F.; Wintgens, V. *Tetrahedron Lett.* **1998**, *39*, 2751–2754.
(23) Nandhikonda, P.; Begaye, M. P.; Heag, M. D. *Tetrahedron Lett.* **2009**, *50*, 2459–2461.
(24) Panchenko, P. A.; Fedorov, Yu. V.; Fedorova, O. A.; Perevalov, V. P.; Jonusauskas, G. *Izv. Akad. Nauk, Ser. Khim.* **2009**, *6*, 1199–1206.
(25) Takahashi, S.; Nozaki, K.; Kozaki, M.; Suzuki, S.; Keyaki, K.; Ichimura, A.; Matsushita, T.; Okada, K. *J. Phys. Chem. A* **2008**, *112*, 2533–2542.
(26) Melhuish, W. H. *J. Phys. Chem.* **1961**, *65*, 229–235.
(27) Lakowicz, J. R. *Principles of Fluorescent Spectroscopy*; Kluwer Academic, Plenum Publishers: New York, 1999; p 53.
(28) Stewart, J. J. P. *J. Mol. Model.* **2007**, *13*, 1173–1213.
(29) Barros, T. C.; Philho, P. B.; Toscano, V. G.; Politi, M. J. *J. Photochem. Photobiol., A* **1995**, *89*, 141–146.
(30) Cho, D. W.; Fujitsuka, M.; Sugimoto, A.; Majima, T. *J. Phys. Chem. A* **2008**, *112*, 7208–7213.

JP9103728